Original Article

# Correlation of Parkinson's disease severity and $^{18}$F-FDG and $^{18}$F-FP-DTBZ PET

**Shuang Li[1,2,3,4], Wei-Zhao Lu[1,3,4], Shao-Zhen Yan[1,3,4], Tian-Bin Song[1,3,4], Chun Zhang[1,3,4], Chang Yang[1,3,4], Jie Lu[1,3,4]**

[1]Department of Radiology and Nuclear Medicine, Xuanwu Hospital, Capital Medical University, Beijing, China; [2]Department of Nuclear Medicine, Xiangyang No. 1 People's Hospital, Hubei University of Medicine, Xiangyang, China; [3]Beijing Key Laboratory of Magnetic Resonance Imaging and Brain Informatics, Beijing, China; [4]Key Laboratory of Neurodegenerative Diseases, Ministry of Education, Beijing, China

*Contributions:* (I) Conception and design: S Li; (II) Administrative support: J Lu; (III) Provision of study materials or patients: TB Song, C Zhang; (IV) Collection and assembly of data: S Li, C Yang; (V) Data analysis and interpretation: WZ Lu, SZ Yan; (VI) Manuscript writing: All authors; (VII) Final approval of manuscript: All authors.

*Correspondence to:* Jie Lu, MD, PhD. Department of Radiology and Nuclear Medicine, Xuanwu Hospital, Capital Medical University, No. 45 Chuangchun Road, Xicheng District, Beijing 100053, China; Beijing Key Laboratory of Magnetic Resonance Imaging and Brain Informatics, Beijing, China; Key Laboratory of Neurodegenerative Diseases, Ministry of Education, Beijing, China. Email: imaginglu@hotmail.com.

**Background:** Positron emission tomography (PET) using the tracer $^{18}$F-fluorodeoxyglucose ($^{18}$F-FDG) and [$^{18}$F] 9-fluoropropyl-(+)-dihydrotetrabenazine ($^{18}$F-FP-DTBZ) is widely utilized to measure metabolic activity and dopaminergic integrity in neurodegenerative diseases such as Parkinson's disease (PD). Previous studies employing $^{18}$F-FDG PET have primarily focused on motor or non-motor symptoms, rather than the severity of PD. This study aimed to measure the glucose metabolism of $^{18}$F-FDG and the dopaminergic function of $^{18}$F-FP-DTBZ across various Hoehn-Yahr (H&Y) stages, analyzing the correlation between metabolic activity, dopaminergic function, and H&Y stages to monitor the severity of PD.

**Methods:** The cross-sectional study recruited 78 PD patients in 3 groups of H&Y stages I, II, and III–V and 18 healthy control (HC) participants to undergo $^{18}$F-FDG and $^{18}$F-FP-DTBZ PET scans. Differences in cerebral metabolism and dopaminergic function between groups were evaluated using Student's *t*-test and Mann-Whitney *U* test. Moreover, Pearson correlation analysis was used to explore the association between cerebral metabolism, dopaminergic function, and H&Y stages in all patients.

**Results:** Patients with PD exhibited significant hypometabolic activity in the frontal cortex and relative hypermetabolic activity in the putamen, globus pallidus, thalamus, and cerebellum when compared to HC individuals ($P<0.05$). Further imaging-clinical correlation research depicted the negative correlation between the metabolic activity in the frontal and putamen regions with H&Y stage. Furthermore, the $^{18}$F-FP-DTBZ binding reductions were 18.6%, 46.6%, and 56.9% for the caudate, anterior putamen, and posterior putamen at H&Y stages I; 36.0%, 56.9%, and 65.9% at H&Y stages II; and 41.2%, 61.9%, and 68.5% at H&Y stages III–V, respectively. The $^{18}$F-FP-DTBZ binding of caudate, anterior putamen, and posterior putamen exhibited significantly negative correlations to H&Y stage.

**Conclusions:** In PD, $^{18}$F-FDG and $^{18}$F-FP-DTBZ PET imaging represent potential biomarkers for tracking metabolic activity and dopaminergic degeneration, offering valuable insights into estimating the severity of disease.

**Keywords:** Parkinson's disease (PD); $^{18}$F-fluorodeoxyglucose ($^{18}$F-FDG); [$^{18}$F] 9-fluoropropyl-(+)-dihydrotetrabenazine ($^{18}$F-FP-DTBZ); positron emission tomography (PET); Hoehn-Yahr stage (H&Y stage)

Submitted Sep 23, 2024. Accepted for publication Feb 04, 2025. Published online Mar 28, 2025.
doi: 10.21037/qims-24-2047
**View this article at:** https://dx.doi.org/10.21037/qims-24-2047

## Introduction

Parkinson's disease (PD) is an age-related neurodegenerative disorder caused by the progressive loss of dopaminergic neurons in the substantia nigra pars compacta (1,2). Neuronal degeneration typically precedes symptom onset in PD by several years, with about 75% of pigmented neurons lost by the time clinical manifestations occur (3). Although the presence of Lewy bodies in the brainstem or cortex serves as a confirmatory sign of PD, the invasiveness and impracticality of this diagnostic method pose challenges (4). Currently, the diagnosis and assessment of disease severity depend heavily on clinical examination and patient follow-up. Various neuroimaging techniques have been developed and implemented in clinical settings to offer more dependable biomarkers for evaluating fundamental features in PD (5-8).

Positron emission tomography (PET) is an *in vivo* imaging modality capable of noninvasively monitoring brain pathophysiological activities in a range of neurological and psychiatric conditions (7). In recent decades, numerous presynaptic dopaminergic imaging methods have concentrated on evaluating nigrostriatal dopaminergic dysfunction using various dopaminergic radiotracers. As per the updated Movement Disorder Society (MDS) clinical diagnostic criteria for PD (9), normal presynaptic vesicular monoamine transporter type 2 (VMAT2) neuroimaging serves as an exclusion to rule out PD. However, VMAT2 imaging has limited utility in distinguishing PD from other atypical parkinsonism due to its lack of specificity (10,11). Additionally, PD involves brain dysfunction beyond dopaminergic deficits. In such scenarios, $^{18}$F-fluorodeoxyglucose ($^{18}$F-FDG) PET has been specifically developed to identify and quantify metabolic abnormalities in PD at the systemic level (12). Both metabolic and dopaminergic imaging have a long-standing tradition in the study of PD (13-15).

The assessment of the severity in dopaminergic and metabolic imaging has been investigated in a limited number of studies (16,17). In addition, these studies did not directly combine assessment of dopaminergic and metabolic imaging with the severity of the disease (18,19). In this study, we aimed to measure the glucose metabolism of $^{18}$F-FDG and dopaminergic function of [$^{18}$F] 9-fluoropropyl-(+)-dihydrotetrabenazine ($^{18}$F-FP-DTBZ) across various Hoehn-Yahr (H&Y) stages, analyzing the correlation between metabolic activity, dopaminergic function, and H&Y stage to identify the severity of disease. We present this article in accordance with the STROBE reporting checklist (available at https://qims.amegroups.com/article/view/10.21037/qims-24-2047/rc).

## Methods

### *Participants*

A total of 78 patients (48 males and 30 females; mean age 57.8±11.7 years) diagnosed with PD by two senior movement disorder specialists following the MDS-PD criteria (20) and who underwent $^{18}$F-FP-DTBZ and $^{18}$F-FDG PET scans at Xuanwu Hospital, Capital Medical University were enrolled in the study between January 2022 and June 2023. The patients were divided into three groups according to the H&Y stage: stage I (n=14, 9 males and 5 females, mean age 60.5±13.5 years), stage II (n=44, 26 males and 18 females, mean age 56.6±12.4 years), and stages III–V (n=20, 13 males and 7 females, mean age 58.5±8.3 years). Additionally, the healthy control (HC) group (10 males and 8 females, mean age 62.5±9.39 years) was included, matching in age, sex, and height with the PD group. The HC participants in our study were recruited during routine health examinations and reported no history of drug abuse, neurological disorders, or psychiatric conditions. This retrospective study was conducted in accordance with the Declaration of Helsinki (as revised in 2013) and received approval from the Medical Research Ethics Committee of Xuanwu Hospital, Capital Medical University (No. [2023]044). The requirement for individual consent for this retrospective analysis was waived.

### *Study design*

Before the examination, PD patients were instructed to discontinue antiparkinsonian medications for at least 12 hours and fast for a minimum of 6 hours, ensuring that their fasting blood glucose levels were below 7.0 mmol/L. Clinical assessment of each patient utilized the Unified Parkinson's Disease Rating Scale (UPDRS) and H&Y stage, categorizing patients into distinct stages based on the H&Y stage. Following the clinical evaluation, all participants underwent $^{18}$F-FDG PET imaging and subsequently $^{18}$F-FP-DTBZ PET the next day, maintaining the same timeframe for both scans. Then, we aimed to measure the glucose metabolism of $^{18}$F-FDG and dopaminergic function of $^{18}$F-FP-DTBZ across various H&Y stages, analyzing the correlations between metabolic activity, dopaminergic

 

function, and H&Y stages to identify regions associated with the severity of disease.

### *PET imaging acquisition*

All participants underwent examination with a hybrid 3.0-T PET/MR scanner (uPMR790, Shanghai, China). For $^{18}$F-FDG PET imaging, scans were conducted 45–55 minutes post-injection (150–200 MBq) and approximately 90 minutes following intravenous injection of $^{18}$F-FP-DTBZ (222 MBq). Parameters: three-dimensional (3D) T1-weighted imaging (T1WI) with a repetition time (TR) of 7.9 ms, echo time (TE) of 2.8 ms, matrix size of 256×256, and voxel dimensions of 1.0 mm × 1.0 mm × 1.0 mm; for PET, ordered subset expectation maximization (OSEM) and time-of-flight (TOF) were employed for reconstruction, with a data acquisition time window of 10 minutes, matrix size of 128×128, slice thickness of 2.44 mm, 4 iterations, 20 effective subsets, and a full width at half maximum (FWHM) of 3.0 mm. All patients were situated in a serene, softly illuminated room for relaxation.

### *Data analysis*

The United Imaging MM BrainAnalysis software (United Imaging, Shanghai, China) was used to analyze $^{18}$F-FDG PET images. Intelligent segmentation based on 3D T1WI was performed, dividing the brain into 106 regions. The segmentation results were then mapped to the $^{18}$F-FDG PET images to extract the mean standard uptake value (SUVmean) for each brain region (21).

Two nuclear medicine physicians with over 5 years of experience analyzed the $^{18}$F-FP-DTBZ PET images collaboratively, using a blinded approach. In cases of disagreement, a third nuclear medicine physician with 10 years of experience made the final assessment. They manually delineated the regions of interest (ROIs) for the caudate nucleus, anterior putamen, and posterior putamen on the layers displayed clearly in the $^{18}$F-FP-DTBZ PET/MRI, measuring the SUVmean. The occipital lobe on the same side was used as the background to calculate the standard uptake value ratio (SUVR) for the ROIs (22,23).

### *Statistical analysis*

Differences in continuous variables [age, age at onset, disease duration, total UPDRS score, UPDRS III score, education, Mini-Mental State Examination (MMSE) and Montreal Cognitive Assessment (MoCA) scores] between groups were evaluated using Student's *t*-test and Mann-Whitney *U* test (2-tailed). Qualitative data were expressed as frequency (percentage) and analyzed using the $\chi^2$ test. For comparisons of the FDG uptake and DTBZ binding between the PD patients and HC participants, an independent samples *t*-test or Mann-Whitney *U* test was performed. One-way analysis of variance (ANOVA) and Kruskal-Wallis rank-sum test (with post hoc pairwise comparisons adjusted using the Bonferroni method) were used to compare the differences in the various H&Y stages (stage I, stage II, and stages III–V) in the caudate and putamen of PD patients. Pearson correlation or Spearman rank correlation analysis was used to evaluate the correlation between FDG uptake and DTBZ binding and various H&Y stages.

## Results

### *Clinical and demographic characteristics*

A total of 78 patients diagnosed with PD participated in the study (H&Y stage I 14 patients, stage II 44 patients, and stages III–V 20 patients), comprising 48 men and 30 women. Their mean age was 57.8±11.7 years, with an average disease duration of 2.97±2.54 years (*Table 1*). There were no significant differences in the demographic data between the PD and HC groups, including gender (P=0.644) and age (P=0.112). In the mild PD group (H&Y stage I), the total UPDRS scores and UPDRS III scores were significantly lower compared to the moderate and advanced PD groups (H&Y stage II and H&Y stages III–V) (P<0.005). Moreover, the education levels in the H&Y stage I were significantly higher than those in the H&Y stages III–V groups (P=0.017). Additionally, the disease duration in the H&Y stage I group was lower than that of the H&Y stages III–V group. No significant differences were observed in the age at onset, MMSE score, and MoCA score among the H&Y stage I, H&Y stage II, and H&Y stages III–V groups (*Table 1*).

### *$^{18}$F-FDG PET results and statistical analysis*

As shown in *Figure 1* and *Table 2*, patients with PD exhibited significant hypometabolic activity in the frontal cortex when compared to age-matched HC individuals (P<0.05). In contrast, relative hypermetabolic activity was observed in the bilateral putamen, globus pallidus, thalamus, and

 

**Table 1** Demographic and clinical characteristics of all participants

| Clinical features | HC | PD | H&Y stage I | H&Y stage II | H&Y stages III–V | P value |
|---|---|---|---|---|---|---|
| Participants | 18 | 78 | 14 | 44 | 20 | |
| Sex (male/female) | 10/8 | 48/30 | 9/5 | 26/18 | 13/7 | 0.644[a] |
| Age (years) | 62.5±9.39 | 57.8±11.7 | 60.5±13.5 | 56.6±12.4 | 58.5±8.3 | 0.112[a] |
| Age at onset (years) | | 55.4±12.3 | 59.9±13.5 | 54.1±13.2 | 55.3±8.6 | 0.177[b]; 0.242[c]; 0.738[d] |
| Disease duration (years) | | 2.97±2.54 | 2.24±1.99 | 2.95±2.75 | 3.53±2.35 | 0.220[b]; 0.089[c]; 0.169[d] |
| Total UPDRS score | | 48.3±21.5 | 37.8±14.9 | 41.1±13.4 | 78.5±15.8 | 0.559[b]; 0.003[c]*; 0.002[d]* |
| UPDRS III | | 27.87±15.3 | 17.83±10.2 | 25.29±10.6 | 44.1±18.3 | 0.043[b]*; <0.001[c]*; <0.001[d]* |
| Education (years) | | 12.10±3.56 | 13.71±2.56 | 12.5±3.22 | 9.88±4.22 | 0.365[b]; 0.017[c]*; 0.086[d] |
| MMSE score | | 27.26±3.3 | 27.00±3.8 | 27.80±2.5 | 26.00±4.5 | 0.395[b]; 0.544[c]; 0.062[d] |
| MoCA score | | 23.44±4.8 | 22.25±6.4 | 24.2±3.9 | 22.4±5.6 | 0.201[b]; 0.948[c]; 0.184[d] |

Data are presented as n or mean ± standard deviation. *, statistically significant differences (P<0.05). [a], comparison among HC and all PD patients. [b], comparison among H&Y stage I and H&Y stage II groups. [c], comparison among H&Y stage I and H&Y stages III–V groups. [d], comparison among H&Y stage II and H&Y stages III–V groups. HC, healthy control; H&Y stage, Hoehn-Yahr stage; MMSE, Mini-Mental State Examination; MoCA, Montreal Cognitive Assessment; PD, Parkinson's disease; UPDRS III, the third part of unified Parkinson's disease rating scale.

cerebellum in PD patients (P<0.05).

The study aimed to examine the relationship between glucose metabolism and H&Y stages. *Figure 2* depicts the negative correlation between the metabolic activity in the frontal (r=–0.227, P=0.046) and putamen (r=–0.244, P=0.031) regions with H&Y stage. In contrast, no significant correlation was observed in parietal, globus pallidus, thalamus, and cerebellum regions.

### *$^{18}$F-FP-DTBZ PET results and statistical analysis*

Significant differences in VMAT2 binding were observed in the caudate and putamen of PD patients at various H&Y stages ($F$=4.479, P=0.015). In a cohort of 14 patients with mild PD (H&Y stage I), $^{18}$F-FP-DTBZ binding was significantly reduced to 18.6% in the caudate, 46.6% in the anterior putamen, and 56.9% in the posterior putamen, compared to HC participants. Among 44 patients with PD at H&Y stage II, striatal $^{18}$F-FP-DTBZ binding demonstrated a significant decrease to 36.0%, 56.9%, and 65.9% respectively, in the corresponding subregions compared to the HC group. Furthermore, in a group of 20 patients with moderate and advanced PD (H&Y stages III–V), $^{18}$F-FP-DTBZ binding was notably reduced to 41.2% in the caudate, 61.9% in the anterior putamen, and 68.5% in the posterior putamen compared to the normal mean. Post hoc analysis revealed that patients with PD exhibited significantly reduced DTBZ binding compared to HC participants (Bonferroni corrected: P<0.05). The most pronounced reduction in $^{18}$F-FP-DTBZ uptake was observed in the posterior putamen, followed by the anterior putamen and the caudate across various H&Y stages. The DTBZ binding in the caudate at H&Y stage I was significantly higher than that in H&Y stage II ($t$=2.46, v=56, P=0.013) and in the III–V groups ($t$=3.12, v=32, P=0.003). In H&Y stages III–V, the $^{18}$F-FP-DTBZ binding in anterior and posterior putamen was significantly reduced compared to that in H&Y stage I (anterior putamen: $Z$=–2.644, P=0.002; posterior putamen: $Z$=–2.486, P=0.003) and stage II (anterior putamen: $Z$=–2.869, P=0.018). Furthermore, the posterior putamen DTBZ binding in H&Y stage II was significantly reduced compared to that in H&Y stage I ($t$=2.507, v=56, P=0.015) (*Figure 3*, *Table 3*).

Furthermore, the investigation was extended to explore the correlation between dopaminergic function in striatal regions and H&Y stages. VMAT2 binding levels in the caudate (r=–0.577, P<0.001), anterior putamen (r=–0.645, P<0.001), and posterior putamen (r=–0.698, P<0.001) were measured, revealing a negative correlation with H&Y stages, as illustrated in *Figure 4*.

## Discussion

PET using $^{18}$F-FDG and $^{18}$F-FP-DTBZ has been

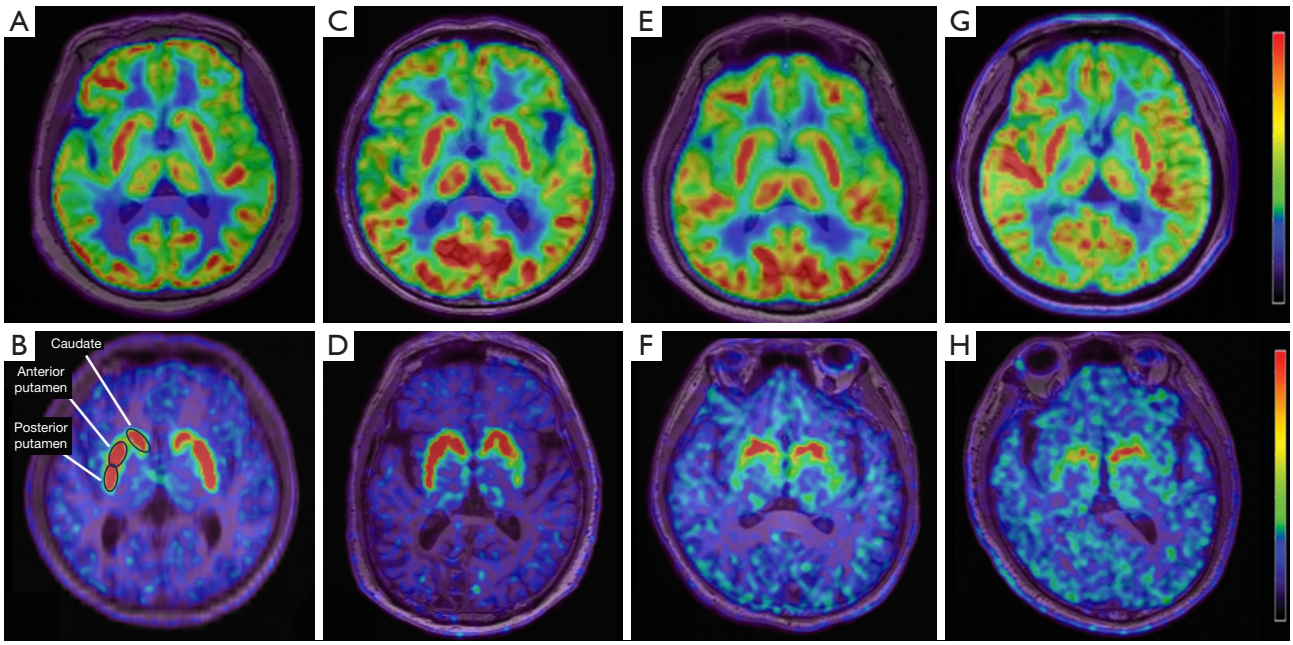


**Figure 1** The $^{18}$F-FDG and $^{18}$F-FP-DTBZ PET/MR imaging in PD patients at various H&Y stages compared to healthy controls**.** (A,B) HC group individual, man, 72 years. (A) $^{18}$F-FDG PET demonstrates a symmetrical distribution pattern across the entire cerebral cortex and nigrostriatal regions, showing no noticeable areas of increased or decreased radioactive uptake. (B) $^{18}$F-FP-DTBZ PET reveals a symmetrical distribution pattern, with the highest uptake in the striatal regions and moderate uptake in the substantia nigra. (C,D) The PD patient at H&Y stage I, woman, 74 years. (C) $^{18}$F-FDG PET exhibited metabolic increase in the putamen. (D) $^{18}$F-FP-DTBZ PET presents a noticeable asymmetric decline in activity in the nigrostriatum, with the greatest loss observed in the posterior putamen. (E,F) The PD patient at H&Y stage II, male, 75 years. (E) $^{18}$F-FDG PET imaging showed metabolic reduction in the frontal cortex. (F) $^{18}$F-FP-DTBZ PET reveals a significant noticeable symmetric decline in putamen. (G,H) The PD patient at H&Y stages III–V, man, 73 years. (G) $^{18}$F-FDG PET imaging showed metabolic reduction in the frontal cortex. (H) $^{18}$F-FP-DTBZ PET reveals a significant noticeable symmetric decline in nigrostriatum. $^{18}$F-FDG, $^{18}$F-fluorodeoxyglucose; $^{18}$F-FP-DTBZ, [$^{18}$F] 9-fluoropropyl-(+)-dihydrotetrabenazine; HC, healthy control; H&Y stage, Hoehn-Yahr stage; PD, Parkinson's disease; PET/MR, positron emission tomography/magnetic resonance.

**Table 2** The SUVmean of $^{18}$F-FDG PET imaging in PD patients and HC individuals

| Region | HC SUVmean | PD SUVmean | H&Y stage I | H&Y stage II | H&Y stages III–V | P value |
|---|---|---|---|---|---|---|
| Frontal cortex | 7.96±1.7 | 6.84±2.4 | 7.37±2.8 | 7.01±2.5 | 6.10±2.0 | 0.027* |
| Parietal cortex | 7.84±1.8 | 6.86±2.2 | 7.12±2.7 | 6.75±2.2 | 6.91±2.0 | 0.050 |
| Temporal cortex | 6.66±1.5 | 6.28±2.0 | 6.32±2.3 | 6.22±2.1 | 6.38±1.8 | 0.335 |
| Globus pallidus | 5.01±0.9 | 6.16±1.7 | 6.02±2.4 | 6.24±1.5 | 6.09±1.6 | 0.005* |
| Putamen | 6.66±0.7 | 8.41±2.9 | 8.83±4.9 | 8.56±2.5 | 7.79±1.8 | 0.012* |
| Thalamus | 6.06±0.8 | 7.03±2.1 | 6.91±2.8 | 7.01±2.1 | 7.20±1.8 | 0.002* |
| Cerebellum | 5.30±0.8 | 6.21±1.8 | 6.10±2.1 | 6.27±1.9 | 6.16±1.6 | 0.038* |

P value indicates the comparison among HC and all PD patients. Data are presented as mean ± standard deviation. *, statistically significant differences (P<0.05). $^{18}$F-FDG, $^{18}$F-fluorodeoxyglucose; HC, healthy control; H&Y stage, Hoehn-Yahr stage; PET, positron emission tomography; PD, Parkinson's disease; SUVmean, the mean standardized uptake value.

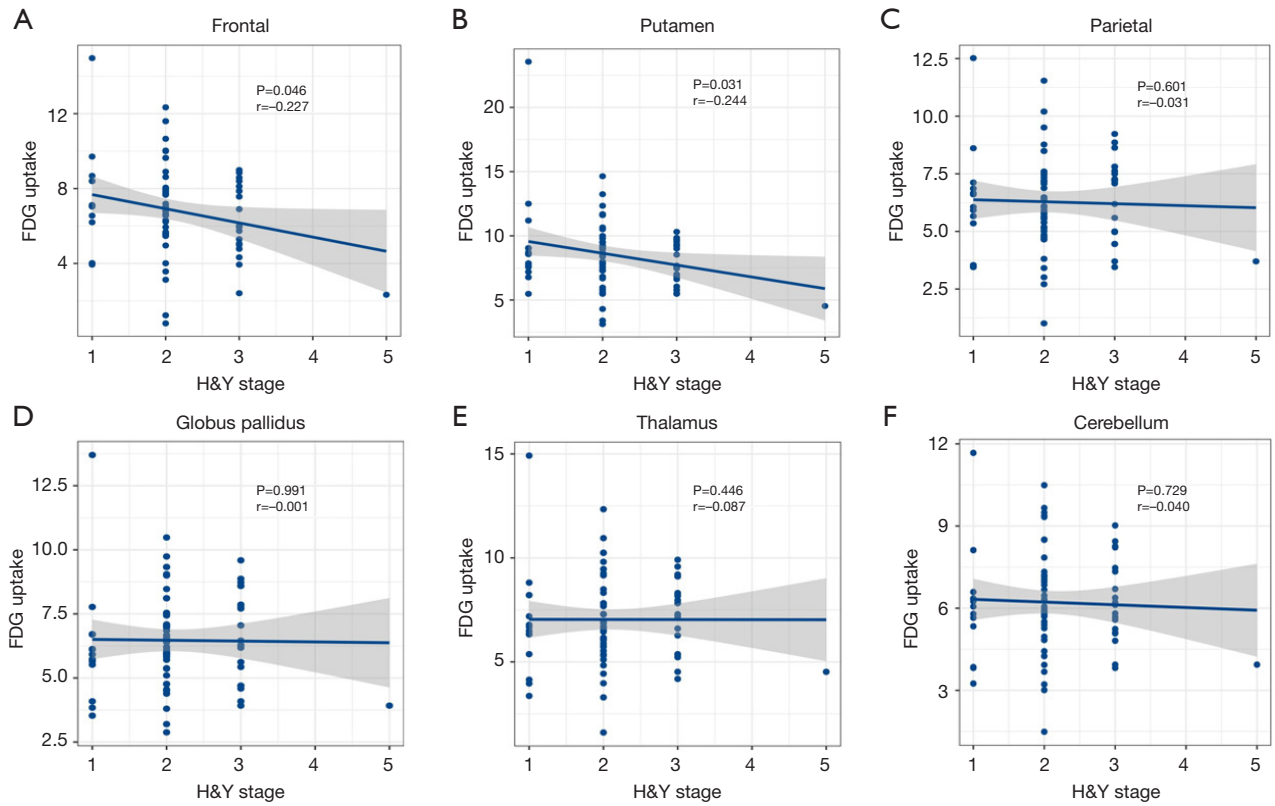


**Figure 2** The correlation between the metabolic activity and H&Y stages. In the frontal (A), the metabolic activity decreased as H&Y stages increased (r=–0.227, P=0.046). Similarly, putamen metabolic activity (B) showed a decrease with increasing H&Y stages (r=–0.244, P=0.031). However, there was no observed correlation in the parietal (C), globus pallidus (D), thalamus (E), and cerebellum (F). FDG, fluorodeoxyglucose; H&Y stage, Hoehn-Yahr stage.

established as a valuable imaging biomarker for measuring metabolic activity and dopaminergic integrity. This study investigated the metabolic activity and dopaminergic function in PD patients across various H&Y stages. Our findings revealed a negative correlation between the metabolic activity in the putamen and frontal cortex, as well as the dopaminergic function in the striatal regions, with the disease severity in PD patients.

The glucose metabolism patterns of patients with PD have been investigated. Eidelberg's research group previously analyzed the presentation of PD-related pattern (PDRP) and observed hypermetabolic activity in the pallido-thalamic and pontine regions, while activity in the supplementary motor area, parietal association areas, and regions of the premotor cortex decreased (24). The elevated metabolic activity in PDRP regions such as the putamen and thalamus showed a direct correlation with standardized motor assessments of patients (25-28). In PD patients, the PD-related cognitive pattern was linked to memory and executive function. This pattern was characterized by decreased metabolism in the medial frontal and parietal areas, along with a relatively hypermetabolic activity in the cerebellar vermis (29,30).

In this study, we found that patients with PD exhibited significant hypometabolic activity in the frontal cortex, along with relative hypermetabolic activity in the putamen, globus pallidus, thalamus, and cerebellum when compared to age-matched HCs. This finding is consistent with previous reports (31). Interestingly, we found a negative relationship between the H&Y stage and glucose metabolism in the frontal cortex and putamen. Specifically, higher H&Y stages were associated with lower metabolic rates in the following regions: frontal: r=–0.227, P=0.046; putamen: r=–0.244, P=0.031. The frontal cortex receives input from the anterior cingulate area, which is a significant site of dopaminergic innervation within the cerebral cortex (32).

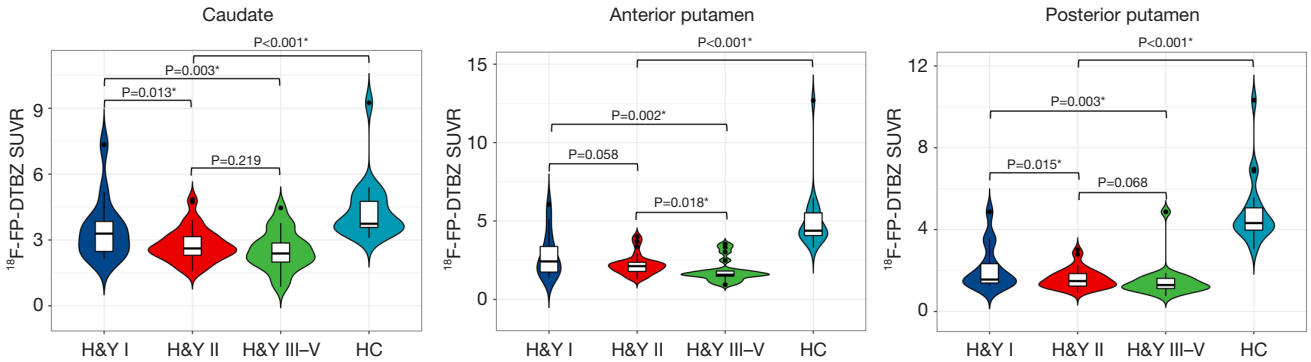


**Figure 3** Comparative analysis of $^{18}$F-FP-DTBZ uptake within the striatum regions in HC individuals and PD patients. The caudate $^{18}$F-FP-DTBZ binding in the H&Y stage I were significantly higher than those in the H&Y stages II ($t$=2.46, P=0.013) and III–V groups ($t$=3.12, P=0.003). The anterior putamen and posterior putamen $^{18}$F-FP-DTBZ binding in H&Y stages III–V were significantly reduce than those in the H&Y stages I (anterior putamen: $Z$=–2.644, P=0.002; posterior putamen: $Z$=–2.486, P=0.003) and II groups (anterior putamen: $Z$=–2.869, P=0.018), and the posterior putamen $^{18}$F-FP-DTBZ binding in H&Y stage II were significantly reduce than those in the H&Y stages I (t=2.507, P=0.015). *, statistically significant differences (P<0.05). $^{18}$F-FP-DTBZ, [$^{18}$F] 9-fluoropropyl-(+)-dihydrotetrabenazine; HC, healthy control; H&Y stage, Hoehn-Yahr stage; PD, Parkinson's disease.

**Table 3** $^{18}$F-FP-DTBZ PET imaging analysis in PD at various H&Y stages

| Region | HC SUVRmean | H&Y stage I | | H&Y stage II | | H&Y stages III–V | | P value |
|---|---|---|---|---|---|---|---|---|
| | | SUVRmean | Decline | SUVRmean | Decline | SUVRmean | Decline | |
| Caudate | 4.30±0.24 | 3.50±0.27 | 18.6% | 2.75±0.81 | 36.0% | 2.53±1.39 | 41.2% | <0.001[a]*; 0.013[b]*; 0.003[c]*; 0.219[d] |
| Anterior putamen | 5.17±0.33 | 2.76±0.23 | 46.6% | 2.23±0.08 | 56.9% | 1.97±0.12 | 61.9% | <0.001[a]*; 0.058[b]; 0.002[c]*; 0.018[d]* |
| Posterior putamen | 4.92±0.26 | 2.12±0.21 | 56.9% | 1.68±0.06 | 65.9% | 1.55±0.12 | 68.5% | <0.001[a]*; 0.068[b]; 0.003[c]*; 0.028[d]* |

Data are presented as % or mean ± standard deviation. *, statistically significant differences (P<0.05). [a], comparison among HC and all PD patients. [b], comparison among H&Y stage I and H&Y stage II groups. [c], comparison among H&Y stage I and H&Y stages III–V groups. [d], comparison among H&Y stage II and H&Y stages III–V groups. $^{18}$F-FP-DTBZ, [$^{18}$F] 9-fluoropropyl-(+)-dihydrotetrabenazine; HC, healthy control; H&Y stage, Hoehn-Yahr stage; PET, positron emission tomography; PD, Parkinson's disease; SUVR, standardized uptake value ratio.

Prior research has demonstrated a link between cognitive decline, behavioral abnormalities, and impaired function in the prefrontal cortex and striatum (33,34). Following deep brain stimulation of the subthalamic nucleus, a linear relationship has been reported between the $^{18}$F-FDG uptake in the frontal lobe and cognitive outcomes, suggesting a potential interaction between the striatum and frontal cortex (35,36).

Consistent with numerous existing $^{18}$F-FDG PET studies, we also observed decreased FDG uptake in the putamen as the H&Y stages advanced. Neurodegeneration of the substantia nigra can lead to abnormal activity in the striatal loop, further exacerbating to the core symptoms of PD (37). A previous functional connectivity (FC) study identified decreased connectivity between the putamen and midbrain regions, including the substantia nigra (38). A similar result was observed in the current study, indicating that decreased FC between the anterior putamen and the substantia nigra is associated with more severe behavioral impairments. This finding demonstrates that reduced connectivity between the putamen and substantia nigra is a reproducible *in vivo* feature indicative of impairment in the nigrostriatal pathway (39). There is a significant interaction effect between iron deposition and nigral-putamen connectivity on putamen FDG uptake, indicating that this joint effect is not substantially influenced by the spatial distribution of FC in the putamen (40). Similar research has reported that caudate glucose metabolism decreased as H-Y stages increased (r=–0.441, P=0.004). In our investigation, both the putamen and frontal cortex exhibited correlations

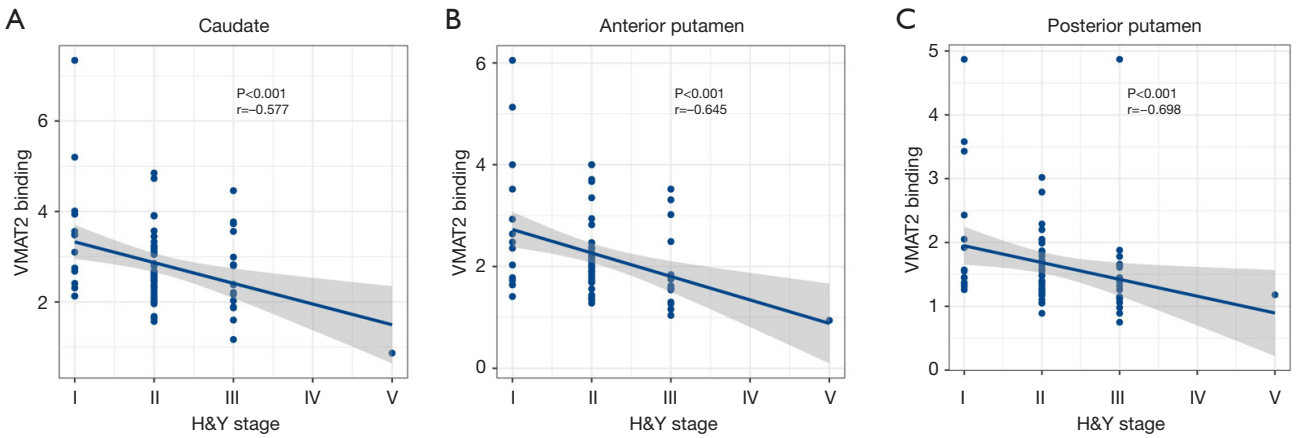


**Figure 4** The relationship between the dopaminergic function in striatal regions and H&Y stages. In the caudate (A), the VMAT2 binding levels decreased as H&Y stages increased (r=–0.577, P<0.001). In the anterior putamen (B), the VMAT2 binding levels decreased as H&Y stages increased (r=–0.645, P<0.001). Similarly, in the posterior putamen (C), the VMAT2 binding levels decreased as H&Y stages increased (r=–0.698, P<0.001). H&Y stage, Hoehn-Yahr stage; VMAT2, vesicular monoamine transporter 2.

with disease severity, suggesting a potential association between cortical and subcortical alterations during the progression of PD.

Biomarkers that enable the early detection of pathological changes prior to the manifestation of clinical symptoms are essential for the advancement of disease modification and treatment planning (41). The activity of presynaptic nigrostriatal neurons can be assessed through imaging of aromatic amino acid decarboxylase, dopamine transporter, and VMAT2. VMAT2 is a specific presynaptic protein that facilitates the transport of monoamines from the cytosol to the storage vesicles of monoaminergic nerve terminals. The density of VMAT2 is linearly correlated with the integrity of dopamine neurons in the substantia nigra (42). In the early stages of PD, AADC, which regulates dopamine synthesis, is upregulated, whereas DAT, which mediates the reuptake of synaptic dopamine, is downregulated. The availability of VMAT2 is relatively unaffected by this compensatory mechanism. Therefore, PET radioligands targeting VMAT2 have been proposed as superior biomarkers for quantifying presynaptic dopamine neurons (43).

Previous imaging investigations on the dopamine systems have linked the loss of dopamine innervations, assessed through various radiotracers such as $^{99m}$Tc-labeled tropane derivatives, $^{18}$F-fluorodopa, $^{11}$C-DTBZ, and $^{18}$F-FP-DTBZ, with clinical severity, especially motor scores of UPDRS (23,44-48). In the current study, $^{18}$F-FP-DTBZ PET imaging reveals a gradual reduction in nigrostriatal binding as the disease advances. VMAT2 integrity was significantly compromised in the posterior putamen, followed by the anterior putamen and caudate among all patients with PD. This finding was consistent with postmortem evidence indicating severe apoptosis of dopaminergic neurons in the lateral ventral tier of the substantia nigra projecting to the putamen. Degeneration of dopaminergic pathways has been shown to be more pronounced in the axonal terminals of the striatum than in the cell bodies of the substantia nigra (23,49-51).

Moreover, the striatal SUVRs were correlated with disease severity, showing the highest decline in $^{18}$F-FP-DTBZ binding for advanced PD and the lowest for mild PD. These findings align with postmortem investigations, which highlight the most significant reduction in dopaminergic innervations occurring in the posterior putamen during more advanced stages of PD (52,53). This consistent pattern was also observed in a prior study using $^{11}$C-DTBZ in patients with PD in early and moderate stages (54). These results suggest that the level of SUVR in striatal regions can offer supplementary insights into the assessment of motor symptom severity in individuals with PD.

This study has several limitations. First, the merging of datasets in the analysis of stages III–V increased the sample size and statistical power, but also introduced heterogeneity among different cohorts. Second, the analysis of FDG uptake using the SUVmean may lead to inaccurate estimates of glucose metabolism. Finally, participants were included based on clinical rather than pathological diagnoses.

## Conclusions

The uptake of FDG in the putamen and frontal cortex, and the uptake of $^{18}$F-FP-DTBZ in striatal regions, demonstrate a strong correlation with the clinical severity of PD. Therefore, $^{18}$F-FDG and $^{18}$F-FP-DTBZ PET imaging represent potential biomarkers for tracking metabolic activity and dopaminergic degeneration, offering valuable insights into estimating the severity of PD.

## Acknowledgments

None.

## Footnote

*Reporting Checklist:* The authors have completed the STROBE reporting checklist. Available at https://qims.amegroups.com/article/view/10.21037/qims-24-2047/rc

*Funding:* This work was supported by the National Key Research and Development Program of China (Nos. 2022YFC2406900 and 2022YFC2406904).

*Conflicts of Interest:* All authors have completed the ICMJE uniform disclosure form (available at https://qims.amegroups.com/article/view/10.21037/qims-24-2047/coif). All authors report that this work was supported by the National Key Research and Development Program of China (Nos. 2022YFC2406900 and 2022YFC2406904). The authors have no other conflicts of interest to declare.

*Ethical Statement:* The authors are accountable for all aspects of the work in ensuring that questions related to the accuracy or integrity of any part of the work are appropriately investigated and resolved. This retrospective study was conducted in accordance with the Declaration of Helsinki (as revised in 2013) and received approval from the Medical Research Ethics Committee of Xuanwu Hospital, Capital Medical University (No. [2023]044). The requirement for individual consent for this retrospective analysis was waived.



## References

1. Tolosa E, Garrido A, Scholz SW, Poewe W. Challenges in the diagnosis of Parkinson's disease. Lancet Neurol 2021;20:385-97.
2. Vijiaratnam N, Simuni T, Bandmann O, Morris HR, Foltynie T. Progress towards therapies for disease modification in Parkinson's disease. Lancet Neurol 2021;20:559-72.
3. Ma SY, Röyttä M, Rinne JO, Collan Y, Rinne UK. Single section and disector counts in evaluating neuronal loss from the substantia nigra in patients with Parkinson's disease. Neuropathol Appl Neurobiol 1995;21:341-3.
4. Dickson DW. Neuropathology of Parkinson disease. Parkinsonism Relat Disord 2018;46 Suppl 1:S30-3.
5. Tian M, Zuo C, Cahid Civelek A, Carrio I, Watanabe Y, Kang KW, Murakami K, Prior JO, Zhong Y, Dou X, Yu C, Jin C, Zhou R, Liu F, Li X, Lu J, Zhang H, Wang J; Molecular Imaging-based Precision Medicine Task Group of A3 (China-Japan-Korea) Foresight Program. International consensus on clinical use of presynaptic dopaminergic positron emission tomography imaging in parkinsonism. Eur J Nucl Med Mol Imaging 2024;51:434-42.
6. Hellwig S, Frings L, Amtage F, Buchert R, Spehl TS, Rijntjes M, Tüscher O, Weiller C, Weber WA, Vach W, Meyer PT. 18F-FDG PET Is an Early Predictor of Overall Survival in Suspected Atypical Parkinsonism. J Nucl Med 2015;56:1541-6.
7. Schröter N, Blazhenets G, Frings L, Jost WH, Weiller C, Rijntjes M, Meyer PT, Brumberg J. Nigral glucose metabolism as a diagnostic marker of neurodegenerative parkinsonian syndromes. NPJ Parkinsons Dis 2022;8:123.
8. Booth S, Park KW, Lee CS, Ko JH. Predicting cognitive decline in Parkinson's disease using FDG-PET-based supervised learning. J Clin Invest 2022;132:e157074.
9. Postuma RB, Berg D, Stern M, Poewe W, Olanow CW, Oertel W, Obeso J, Marek K, Litvan I, Lang AE, Halliday G, Goetz CG, Gasser T, Dubois B, Chan P, Bloem BR, Adler CH, Deuschl G. MDS clinical diagnostic criteria for Parkinson's disease. Mov Disord 2015;30:1591-601.
10. Stoessl AJ, Martin WW, McKeown MJ, Sossi V. Advances in imaging in Parkinson's disease. Lancet Neurol

2011;10:987-1001.
11. Brooks DJ. Molecular imaging of dopamine transporters. Ageing Res Rev 2016;30:114-21.
12. Eidelberg D, Moeller JR, Ishikawa T, Dhawan V, Spetsieris P, Chaly T, Belakhlef A, Mandel F, Przedborski S, Fahn S. Early differential diagnosis of Parkinson's disease with 18F-fluorodeoxyglucose and positron emission tomography. Neurology 1995;45:1995-2004.
13. Perovnik M, Rus T, Schindlbeck KA, Eidelberg D. Functional brain networks in the evaluation of patients with neurodegenerative disorders. Nat Rev Neurol 2023;19:73-90.
14. Simuni T, Chahine LM, Poston K, Brumm M, Buracchio T, Campbell M, et al. A biological definition of neuronal α-synuclein disease: towards an integrated staging system for research. Lancet Neurol 2024;23:178-90.
15. Höglinger GU, Adler CH, Berg D, Klein C, Outeiro TF, Poewe W, Postuma R, Stoessl AJ, Lang AE. A biological classification of Parkinson's disease: the SynNeurGe research diagnostic criteria. Lancet Neurol 2024;23:191-204.
16. Chu JS, Liu TH, Wang KL, Han CL, Liu YP, Michitomo S, Zhang JG, Fang T, Meng FG. The Metabolic Activity of Caudate and Prefrontal Cortex Negatively Correlates with the Severity of Idiopathic Parkinson's Disease. Aging Dis 2019;10:847-53.
17. Beauchamp LC, Dore V, Villemagne VL, Xu S, Finkelstein D, Barnham KJ, Rowe C. Using (18)F-AV-133 VMAT2 PET Imaging to Monitor Progressive Nigrostriatal Degeneration in Parkinson Disease. Neurology 2023;101:e2314-24.
18. Shi X, Yang Y, Jiang L, Chen J, Yi C, Luo G, Wu L, Chu J, Wang J, Chen L, Zhang X. Comparison of 18 F-DOPA and 18 F-DTBZ for PET/CT Imaging of Idiopathic Parkinson Disease. Clin Nucl Med 2022;47:931-5.
19. Li S, Lu W, Yan S, Song T, Zhang C, Yang C, Lu J. The combination of (18)F-fluorodeoxyglucose and (18) F 9-fluoropropyl-(+)-dihydrotetrabenazine positron emission tomography for distinguishing between early-onset and late-onset idiopathic Parkinson disease and analyzing influencing factors. Quant Imaging Med Surg 2024;14:7406-19.
20. Postuma RB, Poewe W, Litvan I, Lewis S, Lang AE, Halliday G, Goetz CG, Chan P, Slow E, Seppi K, Schaffer E, Rios-Romenets S, Mi T, Maetzler C, Li Y, Heim B, Bledsoe IO, Berg D. Validation of the MDS clinical diagnostic criteria for Parkinson's disease. Mov Disord 2018;33:1601-8.
21. Hong Y, Fu C, Xing Y, Tao J, Zhao T, Wang N, Chen Y, You Y, Ren Z, Hong Y, Wang Q, Zhao Y, Yang Y, Zhang J, Xu J, Han X. Delayed (18)F-FDG PET imaging provides better metabolic asymmetry in potential epileptogenic zone in temporal lobe epilepsy. Front Med (Lausanne) 2023;10:1180541.
22. Lin SC, Lin KJ, Hsiao IT, Hsieh CJ, Lin WY, Lu CS, Wey SP, Yen TC, Kung MP, Weng YH. In vivo detection of monoaminergic degeneration in early Parkinson disease by (18)F-9-fluoropropyl-(+)-dihydrotetrabenzazine PET. J Nucl Med 2014;55:73-9.
23. Hsiao IT, Weng YH, Hsieh CJ, Lin WY, Wey SP, Kung MP, Yen TC, Lu CS, Lin KJ. Correlation of Parkinson disease severity and 18F-DTBZ positron emission tomography. JAMA Neurol 2014;71:758-66.
24. Eidelberg D. Metabolic brain networks in neurodegenerative disorders: a functional imaging approach. Trends Neurosci 2009;32:548-57.
25. Lozza C, Baron JC, Eidelberg D, Mentis MJ, Carbon M, Marié RM. Executive processes in Parkinson's disease: FDG-PET and network analysis. Hum Brain Mapp 2004;22:236-45.
26. Eckert T, Van Laere K, Tang C, Lewis DE, Edwards C, Santens P, Eidelberg D. Quantification of Parkinson's disease-related network expression with ECD SPECT. Eur J Nucl Med Mol Imaging 2007;34:496-501.
27. Asanuma K, Tang C, Ma Y, Dhawan V, Mattis P, Edwards C, Kaplitt MG, Feigin A, Eidelberg D. Network modulation in the treatment of Parkinson's disease. Brain 2006;129:2667-78.
28. Meles SK, Renken RJ, Pagani M, Teune LK, Arnaldi D, Morbelli S, Nobili F, van Laar T, Obeso JA, Rodríguez-Oroz MC, Leenders KL. Abnormal pattern of brain glucose metabolism in Parkinson's disease: replication in three European cohorts. Eur J Nucl Med Mol Imaging 2020;47:437-50.
29. Meles SK, Tang CC, Teune LK, Dierckx RA, Dhawan V, Mattis PJ, Leenders KL, Eidelberg D. Abnormal metabolic pattern associated with cognitive impairment in Parkinson's disease: a validation study. J Cereb Blood Flow Metab 2015;35:1478-84.
30. Huang C, Mattis P, Tang C, Perrine K, Carbon M, Eidelberg D. Metabolic brain networks associated with cognitive function in Parkinson's disease. Neuroimage 2007;34:714-23.
31. Seiffert AP, Gómez-Grande A, Alonso-Gómez L, Méndez-Guerrero A, Villarejo-Galende A, Gómez EJ, Sánchez-González P. Differences in Striatal Metabolism

 

in [18F]FDG PET in Parkinson's Disease and Atypical Parkinsonism. Diagnostics (Basel) 2022;13:6.
32. Argyelan M, Carbon M, Ghilardi MF, Feigin A, Mattis P, Tang C, Dhawan V, Eidelberg D. Dopaminergic suppression of brain deactivation responses during sequence learning. J Neurosci 2008;28:10687-95.
33. Apostolova I, Lange C, Frings L, Klutmann S, Meyer PT, Buchert R. Nigrostriatal Degeneration in the Cognitive Part of the Striatum in Parkinson Disease Is Associated With Frontomedial Hypometabolism. Clin Nucl Med 2020;45:95-9.
34. Maiti P, Gregg LC, McDonald MP. MPTP-induced executive dysfunction is associated with altered prefrontal serotonergic function. Behav Brain Res 2016;298:192-201.
35. Kalbe E, Voges J, Weber T, Haarer M, Baudrexel S, Klein JC, Kessler J, Sturm V, Heiss WD, Hilker R. Frontal FDG-PET activity correlates with cognitive outcome after STN-DBS in Parkinson disease. Neurology 2009;72:42-9.
36. Han L, Lu J, Tang Y, Fan Y, Chen Q, Li L, Liu F, Wang J, Zuo C, Zhao J. Dopaminergic and Metabolic Correlations With Cognitive Domains in Non-demented Parkinson's Disease. Front Aging Neurosci 2021;13:627356.
37. McGregor MM, Nelson AB. Circuit Mechanisms of Parkinson's Disease. Neuron 2019;101:1042-56.
38. Rieckmann A, Gomperts SN, Johnson KA, Growdon JH, Van Dijk KR. Putamen-midbrain functional connectivity is related to striatal dopamine transporter availability in patients with Lewy body diseases. Neuroimage Clin 2015;8:554-9.
39. Ruppert MC, Greuel A, Tahmasian M, Schwartz F, Stürmer S, Maier F, Hammes J, Tittgemeyer M, Timmermann L, van Eimeren T, Drzezga A, Eggers C. Network degeneration in Parkinson's disease: multimodal imaging of nigro-striato-cortical dysfunction. Brain 2020;143:944-59.
40. Zang Z, Song T, Li J, Yan S, Nie B, Mei S, Ma J, Yang Y, Shan B, Zhang Y, Lu J. Modulation effect of substantia nigra iron deposition and functional connectivity on putamen glucose metabolism in Parkinson's disease. Hum Brain Mapp 2022;43:3735-44.
41. Brooks DJ, Frey KA, Marek KL, Oakes D, Paty D, Prentice R, Shults CW, Stoessl AJ. Assessment of neuroimaging techniques as biomarkers of the progression of Parkinson's disease. Exp Neurol 2003;184 Suppl 1:S68-79.
42. Xu Y, Tang J, Liu C, Zhao C, Cao S, Yu H, Chen Z, Xie M. MicroPET imaging of vesicular monoamine transporter 2 revealed the potentiation of (+)-dihydrotetrabenazine on MPTP-induced degeneration of dopaminergic neurons. Nucl Med Biol 2021;96-97:9-18.
43. Tang J, Liu C, Liu C, Hu Q, Fang Y, Chen Z. Evaluation of damage discrimination in dopaminergic neurons using dopamine transporter PET tracer [18F]FECNT-d4. EJNMMI Res 2024;14:78.
44. Arjona M, Toldo JMP, Queiroz NC, Pedroso JL, Neto GCC, Barsottini OGP, Felicio AC. A Real-World Study of Cerebral 99mTc-TRODAT-1 Single-Photon Emission Computed Tomography (SPECT) Imaging of the Dopamine Transporter in Patients with Parkinson Disease from a Tertiary Hospital in Brazil. Med Sci Monit 2020;26:e925130.
45. Hsu SY, Lin HC, Chen TB, Du WC, Hsu YH, Wu YC, Tu PW, Huang YH, Chen HY. Feasible Classified Models for Parkinson Disease from 99mTc-TRODAT-1 SPECT Imaging. Sensors (Basel) 2019;19:1740.
46. Morrish PK, Sawle GV, Brooks DJ. An [18F]dopa-PET and clinical study of the rate of progression in Parkinson's disease. Brain 1996;119:585-91.
47. Karimi M, Tian L, Brown CA, Flores HP, Loftin SK, Videen TO, Moerlein SM, Perlmutter JS. Validation of nigrostriatal positron emission tomography measures: critical limits. Ann Neurol 2013;73:390-6.
48. Sanchez-Catasus CA, Bohnen NI, Yeh FC, D'Cruz N, Kanel P, Müller MLTM. Dopaminergic Nigrostriatal Connectivity in Early Parkinson Disease: In Vivo Neuroimaging Study of (11)C-DTBZ PET Combined with Correlational Tractography. J Nucl Med 2021;62:545-52.
49. Tong J, Boileau I, Furukawa Y, Chang LJ, Wilson AA, Houle S, Kish SJ. Distribution of vesicular monoamine transporter 2 protein in human brain: implications for brain imaging studies. J Cereb Blood Flow Metab 2011;31:2065-75.
50. Fearnley JM, Lees AJ. Ageing and Parkinson's disease: substantia nigra regional selectivity. Brain 1991;114 ( Pt 5):2283-301.
51. Damier P, Hirsch EC, Agid Y, Graybiel AM. The substantia nigra of the human brain. II. Patterns of loss of dopamine-containing neurons in Parkinson's disease. Brain 1999;122 ( Pt 8):1437-48.
52. Gibb WR, Fearnley JM, Lees AJ. The anatomy and pigmentation of the human substantia nigra in relation to selective neuronal vulnerability. Adv Neurol 1990;53:31-4.
53. Lehéricy S, Brandel JP, Hirsch EC, Anglade P, Villares J, Scherman D, Duyckaerts C, Javoy-Agid F, Agid Y. Monoamine vesicular uptake sites in patients with

 

Parkinson's disease and Alzheimer's disease, as measured by tritiated dihydrotetrabenazine autoradiography. Brain Res 1994;659:1-9.
54. Bohnen NI, Albin RL, Koeppe RA, Wernette KA, Kilbourn MR, Minoshima S, Frey KA. Positron emission tomography of monoaminergic vesicular binding in aging and Parkinson disease. J Cereb Blood Flow Metab 2006;26:1198-212.

**Cite this article as:** Li S, Lu WZ, Yan SZ, Song TB, Zhang C, Yang C, Lu J. Correlation of Parkinson's disease severity and $^{18}$F-FDG and $^{18}$F-FP-DTBZ PET. Quant Imaging Med Surg 2025;15(4):3036-3047. doi: 10.21037/qims-24-2047